View metadata, citation and similar papers at core.ac.uk
brought to you by CORE
provided by NASA Technical Reports Server

Aircraft Noise Generation and Assessment
Auralization of Air Vehicle Noise for Community Noise Assessment

Stephen A. Rizzi[1] and Abhishek K. Sahai[2]

Abstract This paper serves as an introduction to air vehicle noise auralization and documents the current state-of-the-art. Auralization of flyover noise considers the source, path, and receiver as part of a time marching simulation. Two approaches are offered; a time domain approach performs synthesis followed by propagation, while a frequency domain approach performs propagation followed by synthesis. Source noise description methods are offered for isolated and installed propulsion system and airframe noise sources for a wide range of air vehicles. Methods for synthesis of broadband, discrete tones, steady and unsteady periodic, and aperiodic sources are presented, and propagation methods and receiver considerations are discussed. Auralizations applied to vehicles ranging from large transport aircraft to small unmanned aerial systems demonstrate current capabilities.

Keywords auralization · aircraft community noise

Nomenclature

A	=	tonal amplitude
c	=	speed of sound (m/s)
f	=	frequency (Hz)
M	=	Mach number
p	=	pressure (Pa)
R	=	range (m)
R_a	=	specific gas constant for air (J/(kg K))
K	=	temperature (K)
t	=	time (s)
V_w	=	horizontal wind speed (m/s)
γ	=	adiabatic index
λ	=	acoustic wavelength (m)
φ	=	phase angle (radians)
θ	=	polar emission angle (radians)

Acronyms

DLR	=	German Aerospace Center (Deutsches Zentrum für Luft- und Raumfahrt)
ILR	=	Institute of Aerospace Systems (Institut für Luft- und Raumfahrt), RWTH Aachen
NASA	=	National Aeronautics and Space Administration
NLR	=	National Aerospace Center (Nationaal Lucht- en Ruimtevaartlaboratorium)
ONERA	=	French Aerospace Lab (Office National d'Etudes et de Recherches Aérospatiales)
RWTH	=	Rheinisch-Westfälische Technische Hochschule

[1] Stephen A. Rizzi
NASA Langley Research Center, USA
Stephen.A.Rizzi@nasa.gov

[2] Abhishek K. Sahai
TU Delft, The Netherlands
A.K.Sahai@tudelft.nl

1 Introduction

Auralization is a technique for creating audible sound files from numerical data [1]. Auralization of air vehicle noise can serve several purposes: it provides a means of communicating noise impact to stakeholders in a natural form; it provides feedback to the noise analyst regarding the system under design; and it serves as an integral element of perception-influenced design of new air vehicles [2]. It can be applied to environments interior to the aircraft, e.g., cockpit and cabin, and exterior to the aircraft, e.g., community noise.

Common to any purpose or environment are several elements of auralization. Following a source-path-receiver paradigm, these elements include synthesis, sound propagation, and receiver simulation. Synthesis is the process by which a pressure time history is generated. Propagation conveys the sound from the source to the observer. The synthesis operation may either precede or be subsequent to the propagation operation. If noise synthesis precedes propagation, synthesis is performed at the source and propagation is performed in the time domain. If noise synthesis is subsequent to propagation, propagation is performed in the frequency domain and synthesis is performed at the receiver. Finally, the sound may be additionally prepared for reproduction to a listener in a monaural, binaural or multichannel sense. A simple flowchart depicting the above processes is shown in Fig. 1. Both processing strategies result in an n-channel ($n \geq 1$) pseudo-recording at the receiver suitable for sound reproduction.

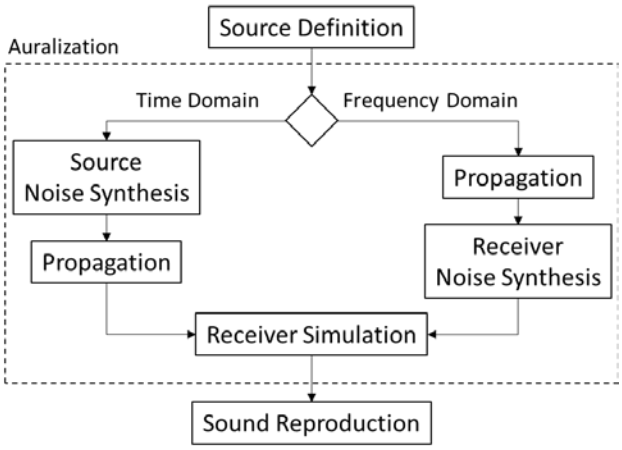

Fig. 1 Flowchart depicting the auralization process in the time and frequency domains.

This paper is concerned with the auralization process itself, with some consideration of its utilization. The intended utilization dictates the level of fidelity required. For example, if the goal of the auralization is to communicate the noise impact of a change in operations or introduction of a new aircraft to the community around an airport, then a high fidelity simulation is required such that the auralization of the current operation or aircraft reflects the experience in the community. However, if the objective of the auralization is to assess the effect of design changes, e.g., installation of a new landing gear, then the auralization should be of sufficient fidelity to determine that change; it need not capture every nuance of the sound or its propagation, e.g., the inclusion of atmospheric turbulence. Rarely is the case that the goal of the auralization is an exact reproduction of a measured flyover.

Although many topics covered herein apply to auralization of interior environments, the focus of this paper is directed at the environment exterior to the aircraft. Section 2 describes time and frequency domain approaches. Section 3 reviews various means of defining the source. Section 4 describes commonly applied synthesis processes. Section 5 discusses time domain propagation, inclusive of path calculation, path dependent propagation effects, and digital signal processing methods. Section 6 addresses receiver simulation and Section 7 considers several applications across a wide spectrum of air vehicles. Finally, this article is intended to serve as an introduction to flyover noise auralization. It is not intended to serve as a comprehensive literature review.

2 Auralization approaches

Auralization of aircraft flyover noise employs a time simulation method wherein the source and receiver attributes (locations, operating conditions, etc.) are evaluated over the course of the event. Because an observer on the ground is not likely to move appreciably over the course of a flyover event, that position is typically considered fixed. In this case, the source emission angle and receiver angle are determined by the instantaneous path between the moving

source and fixed receiver at the time of emission. Samples of sound emitted from a moving source at regular time intervals arrive at a fixed receiver at irregular time intervals. The means for obtaining regularly sampled data at the observer differ between time and frequency domain approaches. Propagation, whether performed in the time domain or the frequency domain, accounts for spreading loss, time delay, atmospheric attenuation and ground reflections.

2.1 Time domain approach

In the time domain approach, sources must be defined either in the time domain (not typical) or be synthesized from a frequency domain description (see Section 4). The source pressure time history is propagated to the receiver through application of an attenuation associated with the spreading loss, a time delay associated with the propagation time, and filters associated with the atmospheric absorption and ground plane impedance. These quantities vary over the course of the simulated event; those variations and their method of application are described in more detail in Sections 4 and 5. The end result of this process is a monaural pseudo-recording with a fixed sampling rate at the receiver. Processing for multichannel receiver simulation and/or generation of noise metrics is optional.

2.2 Frequency domain approach

In the frequency domain approach, sources must be defined either in the frequency domain or converted from the time domain. Propagation in the frequency domain occurs through application of an attenuation associated with the spreading loss, a time delay associated with the propagation time, and spectral modifications associated with the atmospheric absorption and ground plane impedance. The resulting spectral time histories are defined at irregular intervals at the receiver. These may be interpolated to regular time intervals. Alternatively, the source emission time can be selected such that the arrival is at regular intervals. Synthesis of the pressure time history at the receiver follows from the propagated spectrum, with optional processing for receiver simulation and/or metrics.

2.3 Comparison of approaches

From the above, it is clear that either approach should result in the same pressure time history at the observer. However, there are other practical considerations that may make the time domain approach more attractive than the frequency domain approach in some cases. With regard to source noise unsteadiness, the introduction of temporal variations is realizable during synthesis using data or a model of the source noise variation, e.g., jet [3], fan [4] and rotorcraft [5] noise. If the synthesis is performed prior to propagation, then the propagation affects these variations, as is naturally the case. However, if the synthesis is performed at the receiver, that is, after propagation, then the data/model used for source noise unsteadiness must be preconditioned by the propagation effects. Another instance in which the time domain approach might be preferred is for imparting temporal variations in the path, e.g., due to atmospheric turbulence [6]. These may be implemented readily as time varying delays and filters within a time domain propagation approach [7,8], but may be difficult in the frequency domain if the source definition is provided as magnitude only, absent of phase. Related to that, while not fundamentally a constraint, it is often the case that frequency domain propagation is performed on a one-third octave band basis. In doing so, it destroys the phase relationship between direct and ground reflected rays, which negatively impacts the distinctive comb filtering sound associated with a flyover. For the above reasons, the following is mainly focused around the time domain approach.

3 Source noise definition

The source noise must be defined over the duration of the event in either time marching scheme. A brute force approach would necessitate the source characterization for each update interval (or synthesis block as described in Section 4). This is not necessary for flyover events that can be constructed from waypoints that prescribe the aircraft location and operating condition on a larger time scale, e.g., tens of seconds. Therefore, source noise definitions at each waypoint are typically defined a priori at a discrete set of azimuth and elevation (polar) angles at some small fixed radius from the source and are interpolated during the course of the simulation. These sets of coordinates form source ‘hemispheres’ when the range of angles encompass the lower emission angles, or more generally as source ‘spheres.’ The source hemisphere may describe either an isolated source or the installed source, i.e., inclusive of propulsion airframe aeroacoustic (PAA) effects. Note that a sufficient number of waypoints must be specified to capture changes in the source as a function of time, and that the source hemispheres must be sufficiently discretized to capture all of the desired directional attributes. The process is depicted in Fig. 2. For the straight-line path shown, R is the distance between the source and the observer, or slant range.

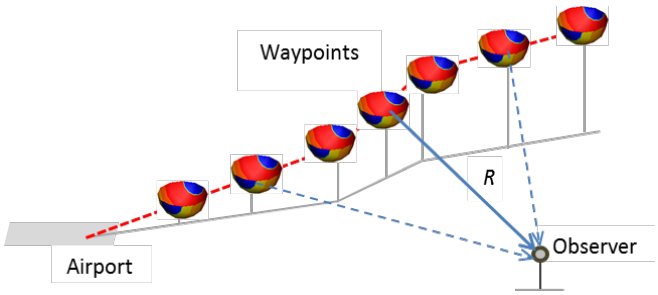

Fig. 2 Aircraft source noise specified at waypoints along a sample flight trajectory.

It is helpful to classify sources according to their type (propulsion system or airframe), component (e.g., fan, jet, and core), method of source noise definition (semi-empirical/analytical, numerical, measurement), and sound classification (e.g., broadband, discrete tones, periodic and aperiodic). Prediction of the entire vehicle noise using high-fidelity computational fluid dynamics (CFD) methods coupled with an acoustic analysis is not feasible with current high-performance computing capabilities. Therefore, the more computationally efficient semi-empirical and analytical methods typically serve as the basis for source noise definitions, or measurements when no predictive capability is available. CFD-based methods are, however, well suited to defining isolated and installed noise sources, predicted at a limited set of steady flight settings. In the context of this work, the broadband sound classification indicates that a broadband amplitude spectrum is specified (typically in 1/3-octave bands), without phase; the discrete tones classification indicates that tonal amplitudes are specified at the harmonics of the blade passage frequency (BPF), without phase; periodic indicates that a pressure time history corresponding to one blade passage or one revolution is specified (note that these can be decomposed into harmonic amplitudes and phases via a discrete Fourier transform (DFT)); and aperiodic indicates that a nonrepeating pressure time history is provided over an extended duration. Consequently, the sound classification effectively dictates the synthesis method, as described in Section 4. Note also that some source noise components apply across different propulsion system or airframe types. For example, gas turbine core noise applies to turbojet, turbofan, turboprop, and turboshaft engines.

In the following, an inventory of common source noise components particular to propulsion systems and airframes, and their associated method of source noise definition and sound classification, are offered in Sections 3.1 and 3.2, respectively. Incorporation of installation effects and noise treatments are discussed in Section 3.3, and system noise prediction in Section 3.4.

3.1 Propulsion System Noise

First, consider gas turbine engine source noise components typically included in auralizations of large aircraft flyover noise. Common to all gas turbine engines are the core noise components provided in Table 1. The core noise describes all noise associated with the compressor, combustor, and turbine. It should be noted that the methods indicated here and in subsequent instances refer to those that are computationally expedient and typically used for auralization. Specific methods are indicated in the examples offered in Section 7. Higher fidelity noise prediction methods are usually employed for other purposes, e.g., development of noise reduction technologies. The reader is directed to the papers on propulsion system noise prediction found in this special issue and in reference [9] for additional information.

Table 1 Core noise components common to gas turbine engines.

Component	Typical Source Noise Method	Classification
Compressor (see Fan, Table 2)	Semi-empirical / Freq. Domain	Broadband, Discrete Tones
Combustor	Semi-empirical / Freq. Domain	Broadband
Turbine	Semi-empirical / Freq. Domain	Broadband, Discrete Tones

In addition to the above, noise components typically included in the auralization of turbojet and turbofan engines are provided in Table 2. The fan noise components are, of course, only associated with turbofan engines and the balance between jet and fan noise components is dependent on the bypass ratio; typically the higher the bypass ratio, the lower the jet noise and higher the fan noise. Fore- and aft-radiated fan noise sources are often treated as separate components within an auralization so that different treatments may be applied to each (see Section 3.3). The jet noise components include mixing noise and broadband shock noise. Jet screech tones are typically avoided in the design and are therefore normally neither predicted nor auralized.

Note that prediction methods are usually less developed for the most recent technologies. In the absence of a reliable prediction method, the auralizations may be based on ground test data acquired at model or full scale. Because the measurements typically include both broadband and discrete tones, added steps are needed for source noise separation, e.g., as described by Rizzi et al., for the fan noise associated with a geared turbofan engine [10].

Table 2 Noise components common to auralization of turbojet and turbofan engines.

Component	Typical Source Noise Method	Classification
Jet: Mixing noise	Semi-empirical / Freq. Domain	Broadband
Jet: Broadband shock noise (supersonic only)	Semi-empirical / Freq. Domain	Broadband
Fan: Broadband	Semi-empirical / Freq. Domain	Broadband
Fan: Rotor-stator interaction noise	Semi-empirical / Freq. Domain	Discrete Tones
Fan: Multiple-pure tones / combination tones ('buzz saw')	Semi-empirical / Freq. Domain	Discrete Tones

Propfan engines (including turboprops, unducted turbofans, open rotor engines, etc.) and turboshaft engines commonly used for rotorcraft typically add a gearbox and possibly a transmission. Propfan engines can operate in either a tractor or a pusher configuration. For both the propfan and turboshaft engines, the associated propeller or rotor noise is typically dominant over the gearbox, transmission and exhaust noise for observers on the ground.

Propeller noise consists of thickness and loading noise components and a broadband noise component, and may be steady periodic, unsteady periodic, or aperiodic. Steady periodic noise is generated for a clean, zero inflow angle and may be predicted analytically under some conditions, but more usually is computed numerically in the time domain. Unsteady periodic noise is generated when the propeller experiences a repeated loading over the course of a revolution, e.g., for a nonzero inflow angle. Unsteady periodic noise can also be generated when propellers operate in multiple rows of blades. The contrarotating open-rotor (CROR) design consists of two rows of propellers, with the aft row moving in the opposing direction to the forward row to remove spin and enhance thrust. Periodic and broadband noise associated with CROR designs differs from that of a single row of propellers due to the interaction between the forward and aft blades. If defined by ground test measurements, CROR noise, like geared turbofan noise, requires discrete tone and broadband source noise separation [11]. Aperiodic loading and thickness noise, and trailing edge noise occur under random inflow conditions. Due to the short duration of numerical simulations, the use of such data for a full flyover remains to be investigated. The propeller noise components are summarized in Table 3.

Table 3 Propeller noise components common to auralization.

Component	Typical Source Noise Method	Classification
Steady loading & thickness noise	Analytical / Freq. Domain	Discrete Tones
Steady loading & thickness noise	Numerical / Time Domain	Periodic
Unsteady loading & thickness noise	Numerical / Time Domain	Periodic, Aperiodic
Steady trailing edge noise	Semi-empirical / Freq. Domain	Broadband
Unsteady trailing edge noise	Numerical / Time Domain	Aperiodic

Rotor noise consists of thickness and loading noise, blade-vortex interaction (BVI) noise (a form of unsteady loading noise), high-speed impulsive noise, and broadband noise produced by turbulence, blade-wake interactions (BWI) and self-noise [12]. The same sources largely apply to tail rotors, except for high-speed impulsive noise, BVI, and BWI noise. The rotor noise components are summarized in Table 4. Less conventional configurations, e.g., compound helicopters, introduce additional interactions. It is often the case that rotorcraft noise is defined through flight test measurements. In such cases, the ground recordings must be back propagated to the source (see the acoustic repropagation technique [13]) to remove spreading loss and Doppler shift, then separated into individual rotor components (e.g., main and tail) [14], yielding a time-averaged representation of the steady and unsteady thickness and loading noise.

Finally, little work has been done in the aviation sector to characterize the noise from reciprocating engines employed in general aviation and small helicopter aircraft. There is likely much that can be gained from the automotive industry in this area. Similarly, a model for electric motor noise is needed for a more complete auralization of the small-medium unmanned aerial systems (UAS) and urban air mobility (UAM) sectors of the emerging aviation market.

Table 4 Rotor noise components common to auralization.

Component	Typical Source Noise Method	Classification
Steady loading & thickness noise	Numerical / Time Domain	Periodic
BVI noise	Numerical / Time Domain	Periodic
High-speed impulsive noise	Numerical / Time Domain	Periodic
Broadband noise	Semi-empirical / Freq. Domain	Broadband

3.2 Airframe Noise

Because of the advances made in lowering turbofan noise, largely through introduction of higher bypass ratio engines, the airframe noise associated with modern large commercial transports can exceed the engine noise on approach. Auralization of these components is thus required for any utilization. A summary of major airframe noise components common to large commercial transports is provided in Table 5. Each of these sources is considered as broadband. Less commonly included broadband noise components for large commercial transports are associated with control surfaces, e.g., ailerons and spoilers. Tonal noise sources, such as fuel vents and cavities in the airframe, have not been included in most source noise models, though their addition could yield higher fidelity auralizations. As was the case for propulsion system noise, the short duration of numerical simulations make the use of such data for full flyover auralizations challenging.

Table 5 Major airframe noise components common to auralization of large commercial transports.

Component	Typical Source Noise Method	Classification
Landing gear noise: Main and nose	Semi-empirical / Freq. Domain	Broadband
Trailing edge flap noise	Semi-empirical / Freq. Domain	Broadband
Leading edge slat noise	Semi-empirical / Freq. Domain	Broadband
Trailing edge noise: Wing and tail	Semi-empirical / Freq. Domain	Broadband

Although the component sources and methods are applicable to other vehicle classes, e.g., rotorcraft and GA aircraft, auralization of airfrane noise components for these vehicles is not typically included as it is not a dominant source, even on approach.

3.3 Installation Effects and Noise Treatments

The last two subsections considered propulsion system and airframe noise sources in isolation. Installation of the propulsion system on the airframe introduces PAA effects, which include both aerodynamic and acoustic effects. Aerodynamic effects modify the source noise generation, e.g., the effect of a pylon on a pusher propeller design. Acoustic effects modify the noise propagation, e.g., acoustic shielding of engine sources on a hybrid wing body configuration. While many installations have the detrimental effect of increasing the noise of the installed source relative to the isolated source, installation effects can be beneficial when incorporated in the development of noise reduction strategies and treatments.

The introduction of installation effects and/or noise treatments thus modifies the isolated source definition. The modification may be incorporated within the source noise definition itself, or may come in the form of a directionally dependent suppression table that is subsequently applied to the isolated source. In either case, the source noise definition ultimately serving as input to the noise synthesis reflects the modified source.

Some common installation effects and noise treatments are indicated in Table 6. The list is not exhaustive, but rather is intended to provide the reader with a sense of how these effects may be included in an auralization. Acoustic liners have been employed for many years as a noise treatment to reduce forward and aft radiated discrete tone and broadband noise. The effect of liners may be realized through application of a suppression table. The placement of the engine relative to the wing has been shown to have a significant effect on the engine noise reaching a ground observer. In conventional under-the-wing engine installations, all engine noise except for forward radiated fan noise is increased due to reflections off the wing and flaps. The acoustic effects of this installation can often be assessed through geometrical acoustic modeling. Novel configurations, like the hybrid wing body (HWB) and over-the-wing engine installations, introduce more complicated aerodynamic and acoustic shielding effects. Such configurations often require a more sophisticated means of assessment, e.g., wind tunnel experiments [15] and/or CFD. Chevrons, noise treatment devices applied to the core nozzle and/or bypass duct, can reduce jet noise through enhanced mixing. Within the auralization process, chevrons may be accounted for through application of a suppression table, which reduces the isolated jet noise in a manner particular to the installation. Finally, the proximity of propellers and rotors

to nearby airframe structure can greatly increase the harmonic content of the generated noise. In a pusher configuration, the wake of the pylon introduces an unsteady periodic loading on the propeller blades, which increases the high frequency content of the noise relative to the isolated source. In a tractor configuration, the presence of a nearby wing may modify the inflow angle. Airframe structures mounted above or below a rotor may similarly influence the blade loading, or cause the unsteady loading on the structure to radiate noise [16]. In the above cases, CFD analyses are usually required to obtain the unsteady loading on the propeller/rotor blades and nearby structure, that serve as input to the acoustic calculation.

Table 6 Common installation effects and noise treatments, and the associated components affected.

Installation Effect/Noise Treatment	Source Component Affected
Inlet acoustic liners	Forward radiated fan noise
Aft bypass duct acoustic liners	Aft radiated fan noise
Engine placement	Many engine components
Chevrons	Jet noise
Propeller/rotor-structure interaction	Propeller/rotor noise, airframe structure

3.4 System Noise Prediction

The source noise definition is often performed within the context of a system noise prediction tool such as the NASA Aircraft Noise Prediction Program (ANOPP) [17] and ANOPP2 [18], the DLR Parametric Aircraft Noise Analysis Module (PANAM) [19], and the ONERA CARMEN acoustic model [20], among others. These tools cannot auralize the noise, but often have the capability to predict the aircraft noise as the sum of its individual components, including those associated with the propulsion system, the airframe, and their installation effects and noise treatments. For that purpose, however, additional information is needed. Flight profiles in trimmed states must be ascertained from data describing the system, e.g., engine operating limits, airframe geometric definition, and aircraft weight. Some tools developed for this purpose include, for fixed wing: the ILR's MICADO [21], the NASA Flight Optimization System (FLOPS) [22], and the flight mechanics module in the TU Braunschweig Preliminary Aircraft Design and Optimization (PrADO) [23] tool. The Comprehensive Analytical Model for Rotorcraft Aerodynamics and Dynamics (CAMRAD-II) [24] code serves this purpose for rotary wing aircraft. See also the system level assessment papers in this special issue.

For gas turbine driven aircraft, the system noise prediction programs also require detailed gas turbine cycle inputs based on the engine's operational state as well as geometrical inputs specifying the engine component geometry. Various gas turbine simulation programs such as the NASA Numerical Propulsion System Simulation (NPSS) environment [25], the NLR Gas turbine Simulation Program (GSP) [26], and the RWTH Aachen University GasTurb program [27] have been employed for this purpose.

The system noise prediction may be performed in standalone fashion. It may also be part of a more comprehensive aircraft simulation program, e.g., PrADO or MICADO of ILR, which incorporates the Integrated Noise Simulation and Assessment (INSTANT) module [28]. It may also be part of a general-purpose, integrated multidisciplinary optimization tool, e.g., OpenMDAO [29], or a vehicle class-specific optimization tool, e.g., the NASA Design and Analysis of Rotorcraft (NDARC) [30] program for rotorcraft.

Finally, while the content of this section has been geared primarily to source noise description for the time domain auralization approach, there are other simulation tools available which generate a receiver noise description suitable for use in the frequency domain auralization approach. These tools are essentially propagation codes that read externally generated source noise hemispheres and propagate those along a simulated trajectory to the receiver, e.g., the Advanced Acoustic Model (AAM) [31].

4 Synthesis

In the context of the time domain auralization approach, the goal of the synthesis operation is to generate a pressure time history at the moving source along an emission angle that varies with time. The entire process for a single time increment of time domain auralization is depicted in Fig. 3. A fixed observer position is assumed. The scenario, comprised of the aircraft operating condition, position and orientation, is first updated. Next, the instantaneous path between each source and observer at the time of emission is determined, as described in Section 5. The path describes the source emission angle, the listener receiver angle (if receiver effects are incorporated), and the set of points between source and receiver required to define the path. Here, a source may refer to a single component, e.g., forward-radiated fan noise, or a group of acoustically collocated components, e.g., the left engine, that share a common path. More

than a single path exists per component/source in the presence of a ground plane or other reflecting surface. The source emission angle is used with the source description to synthesize a short sample of noise. This operation is performed in such a way to smoothly transition between emission angles, as described below for different sound classifications. The resulting sample buffer is propagated to the receiver and accumulated in an output buffer, which may be summed across multiple sources and paths. The propagation uses the gain, time delay and filter associated with the path traversal, as described in Section 5. The process depicted in Fig. 3 is typically performed at a short update interval, 5-10 ms, to allow for changes to the source and propagation path with time. The number of samples in the interval is referred to as the 'hop' size, and is usually on the order of 256-512 samples at an audio sampling rate of 44.1 kHz. With these processing steps in mind, the synthesis technique for each classification type (broadband, discrete tones, periodic and aperiodic) is next explained.

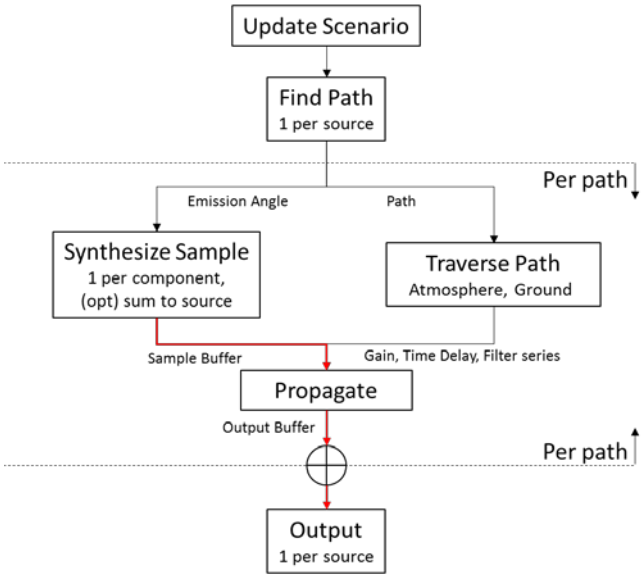

Fig. 3 Flowchart detailing steps in the time domain auralization process. Black connecting lines indicate data and red connecting lines indicate audio samples.

4.1 Broadband Sources

The synthesis of broadband sources is generally performed as a subtractive synthesis operation, that is, a process which starts with a broadband white noise signal and subtracts from it spectral amplitudes through a filtering operation. It makes use of an Overlap-Add (OLA) technique to smoothly vary the generated signal across each hop. A flowchart depicting the steps is indicated in Fig. 4.

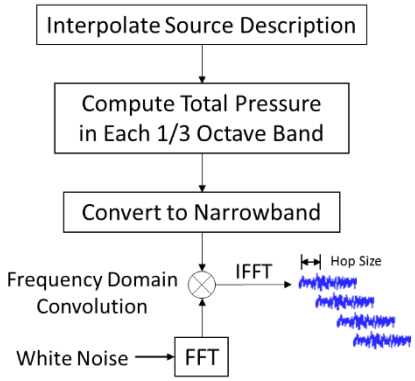

Fig. 4 Flowchart depicting broadband synthesis process.

The first step in this process is interpolation of the instantaneous 1/3-octave band source noise description. This interpolation is performed individually for each 1/3-octave band across two spatial dimensions (between azimuth and

elevation angles) and one temporal dimension (between waypoints). The conversion of the interpolated source to a narrowband spectrum involves evenly distributing the total pressure within each 1/3-octave band over the number of evenly distributed narrowband bins within that band. Although the semi-empirical frequency domain prediction methods provide information on the frequency distribution and amplitudes of the broadband noise components, they do not provide any information on the phase. Therefore, random phase must be assigned for the Inverse Fast Fourier Transform (IFFT) to the time domain. This may be accomplished via a frequency domain convolution with white noise as depicted in Fig. 4, or by simply assigning a random phase to each narrowband frequency component. The result is a complex function that, when inverse transformed, generates the pressure time history. The size of the complex function, referred to as the FFT block size, is selected to be greater than the hop size. The next block of samples to be processed corresponds to a later emission point in the trajectory. To avoid audible artifacts when transitioning from update to update, the blocks are not processed in a contiguous manner, but rather with an overlap with the preceding block(s). The output of each operation is windowed, e.g., using a Hann window, and added to that of the previous block(s) with a time offset corresponding to the hop size. The combination of the FFT block size and the hop size determines the amount of overlap. The synthesized signal transitions smoothly for any changes in the source noise directivity with respect to the observer as well as any operational changes along the flight trajectory.

Two exceptions to the above process are noted. The first exception has to do with the fact that some of the noise prediction models incorporate Doppler shift within the source noise description. Because Doppler shift is imparted during auralization as part of propagation process (see Section 5), it must be removed prior to the synthesis. The removal of the Doppler shift is performed using the relation

$$f^{i} = f^{i}_{Doppler}\left(1 - M\cos\theta\right) \tag{1}$$

in which f refers to the non-Doppler shifted frequency, $f_{Doppler}$ to the Doppler shifted frequency (as output from the source noise prediction model), M to the aircraft Mach number and θ to the polar directivity emission angle. The removal of the Doppler shift is performed prior to the narrowband spectral division, with the division then carried out between the lower and upper non-Doppler shifted frequencies for each of the i^{th} bands. The second exception has to do with the incorporation of temporal variations in the source. These may be applied as time dependent variations about each 1/3-octave band amplitude following the interpolation of the source description, e.g., see ref. [3].

Lastly, if the source description is provided directly in narrowband form, then the synthesis process follows Fig. 4, skipping the conversion to narrowband, e.g., see the broadband synthesis for open rotor noise in ref. [11].

4.2 Discrete Tones

Due to the very different nature of discrete tonal noise compared to broadband noise, a different synthesis approach is followed. Specifically, an additive synthesis technique is used. This technique is performed in the time domain and may be applied to any discrete tone source identified in Table 1-Table 3. The pressure time history for each tone is represented as an amplitude- and frequency-modulated cosine wave, according to the following relations

$$p_k(t) = A_k(t)\cos\left(\varphi_k(t) + \varphi_o\right) \tag{2}$$

$$\varphi_k(t) = 2\pi\int_0^t f_k(\tau)\mathrm{d}\tau \tag{3}$$

in which A_k is the amplitude, φ_k is the instantaneous phase and φ_o is the initial phase of the k^{th} tone. Recall that our definition of a discrete tone source is one in which the tonal amplitudes are specified at the BPF harmonics, without phase. Note that Eqs. (2) and (3) can, as well, be applied to nonharmonically related sources. In the absence of any other information, the initial phase is typically assumed to be random; an exception for buzz saw noise is noted below. The relation between the instantaneous phase φ_k to the instantaneous frequency f_k of each tone is shown in Eq. (3). This form allows the frequencies to change with time, e.g., an engine spool-up. If the specified tone frequencies are Doppler shifted, then an approach similar to that shown by Eq. (1) can be followed to remove the Doppler shift.

The additive synthesis method does not rely on an OLA technique to produce a smoothly changing pressure time history with changes in emission angle and operating condition. Instead, a sample buffer corresponding to the hop size is generated for tonal frequency. Continuity between hop boundaries is achieved by maintaining phase between subsequent hops, even when the instantaneous frequency changes with time due to changes in operational state. All harmonics for a given component are summed to obtain the total tonal noise for that component.

Exceptions to the above are noted for fan buzz saw noise. The typical semi-empirical source noise method specifies this component as a broadband type. Therefore, in order to generate tones, the 1/3-octave band source noise description first needs to be converted to tonal amplitudes. The process is analogous to that used to convert broadband to narrowband, but here the total pressure is divided evenly by the number of buzz saw tones in each band. These are determined not at the BPF, but at integer multiples of the engine low pressure shaft speed (*N1*); the BPF is equal to

N1 times the number of fan blades. Dedopplerization may be required depending on the method used. In different applications, a random phase was assigned (see ref. [32]), or the alternating phase associated with the archetypal saw tooth waveform was assigned (see ref. [33]).

Another exception to the above comes with the introduction of temporal variations. Allen et al. developed a method for characterizing and applying low frequency variations in amplitude and frequency using ground test data from an isolated fan [4]. These were imparted during synthesis by modeling the amplitude and instantaneous frequency of each component as a time-invariant mean plus a time-varying fluctuation.

4.3 Steady and Unsteady Periodic Sources

Synthesis of periodic component noise follows a similar methodology as discrete tones and applies to both steady and unsteady source. The source noise description in this case is a pressure time history at each point on the source hemisphere having a minimum duration of one period. In the trivial case of a stationary source at one of the computed emission angles, the source noise synthesis amounts to simple replication of the prediction over its period. However, any nontrivial case entails synthesis at other emission angles, and therefore, requires some form of interpolation. A straightforward means of doing so is in the frequency domain. The synthesis process thus entails:

i. Analyze the pressure time history at each prediction point using a DFT over the period of one blade passage, e.g., the period of a two-bladed propeller/rotor corresponds to half a revolution. Each spectral line is a harmonic of the BPF.
ii. Compute the magnitude A and phase φ_o for each harmonic at all prediction points from the real and imaginary parts of the DFT.
iii. Interpolate magnitude/phase to the instantaneous emission angle.
iv. Synthesize a hop size buffer according to Eqs. (2) and (3).
v. Repeat steps iii and iv until complete.

Note that the time increment of the source definition is independent of the synthesis time increment. This allows the above approach to simultaneously synthesize and resample the source from a typically lower prediction sampling rate to the higher audio sampling rate. Variations on a theme include the introduction of a time-varying amplitude and phase, in a process akin to that used for fan noise. A model of amplitude variations derived from measured rotorcraft flyover noise is a recent example of such an approach [5].

An alternative approach to the above is to eliminate the discrete source noise description on the hemisphere. This is possible when the source description is obtained from a time domain prediction using computed blade loadings and Farassat acoustic formulation F1A [34]. Instead of computing the pressure time history for a full period at each observer point, it is possible to synthesize sample by sample the pressure time history for a changing emission angle. This F1A synthesizer has the advantage of computing the acoustic pressure only when and where needed, but comes at the cost that it binds the acoustic prediction/synthesis to a specific source-observer pair for a specific flyover trajectory.

4.4 Aperiodic Sources

Aperiodic sources are unsteady by definition. There is no repetition of the pressure time history from an aperiodic source. Unsteady sources may have both broadband and tonal components. It is impractical to compute the unsteady pressure time history of any source for the duration of a flyover. If this were possible, then an approach similar to the F1A synthesizer could be implemented. Instead, aperiodic sources may be handled in one of two ways; both rely on a sufficient record length of data for analysis and a means of separating broadband and tonal noise. With the sources separated, it might be possible to use data to develop new semi-empirical broadband and discrete tone models across a range of model parameters. A comprehensive data set for such an endeavor is an expensive undertaking, whether the data were numerically generated or experimentally acquired. A more direct approach is to synthesize the broadband and discrete tonal sources directly from test data, as was done for the open rotor [11] and geared turbofan [10] components. Either the direct or modeled approach would require an added step of imparting the temporal variations otherwise lost in the process. The authors are unaware of any published work based on either approach.

5 Propagation

Before the sound from the aircraft reaches an observer on the ground, it undergoes several propagation effects that modify its amplitude and spectral content. The primary propagation effects that aircraft noise undergoes as it propagates through the atmosphere are those of geometric or spherical spreading, atmospheric absorption, and

propagation time delay, the time rate of change of which corresponds to the Doppler shift. Additionally, reflection and attenuation from the ground plane or other surface need to be taken into account. In the following, each source (collection of acoustically collocated components) is assumed to be compact and may be treated as a point source if the maximum acoustic source dimension L meets the following criteria [35]

$$L \ll R_{\min} \qquad L \ll \frac{\lambda}{\left|1 - M\cos\theta\right|} \tag{4}$$

in which $R_{\min}$ is the minimum distance between the source and observer and λ is the shortest wavelength of interest. By this definition, each source has its own propagation path(s) and hence its own propagation effects. However, the entire aircraft, comprised of multiple sources, is often handled as a single source located at the origin of the body axis. The following subsections discuss three operations associated with propagation, namely, the path calculation, the path traversal through which the gain, time delay and filters are established, and the application of these to the synthesized signal, see Fig. 3.

5.1 Path calculation

The first step in the propagation process, and in the auralization process itself, is to establish the path. As previously noted, the path describes the source emission angle (needed for synthesis), the listener receiver angle (if receiver effects are incorporated), and the set of points between source and receiver required to traverse the path to establish propagation effects. The path is (re)calculated with each update of the scenario, that is, at the hop interval. We start with the straight-line path case (no refraction), then briefly consider the more-complicated curved path case (with refraction).

5.1.1 Straight-Line Path

A straight-line path exists only in a homogeneous (zero-wind and constant temperature) atmosphere having a constant speed of sound c. It is a good approximation to the more complicated curved path for short ranges, e.g., near the airport environment, and at overhead angles [36]. The straight-line path calculation is purely a geometrical one and is determined for the source location at the emission time [3,36,37]. It is independent of the speed of sound. The source emission and reception angles for the direct path constitute alternate interior angles. Only two points are required to define the direct path; the source and receiver locations. There may be additional path(s) associated with specular reflections off of a surface; the ground is most common surface for flyover auralization. Note that diffuse reflections are not normally considered. The indirect or reflected paths are often determined using an image source [3,38], as shown in Fig. 5. The path for a ground reflected source is defined by three points; the source and receiver locations, and the reflection point on the ground. These are effectively collapsed to two points using an image source. For an observer near the ground, the emission angle for the direct and ground reflected path is generally considered the same, indicating that the source is synthesized once and propagated twice.

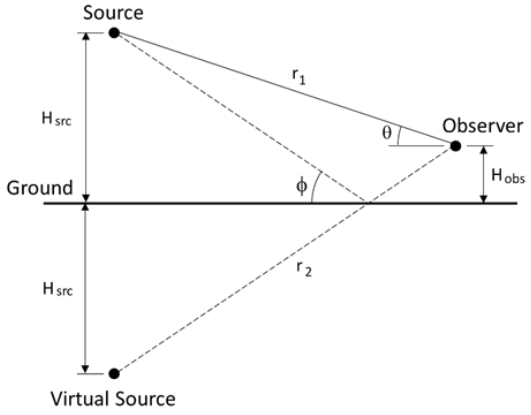

Fig. 5 Image source for ground reflected path.

5.1.2 Curved Path

Gradients in the speed of sound due to wind and temperature gradients cause refraction or a curvature of the propagation path. The set of points defining the path are typically determined with a ray-tracing approach [36] using Snell's law to compute angle of refraction at the interfaces of a layered atmosphere based on the angle of incidence

and the indices of refraction above and below the interface. The latter depends on the effective speed of sound given by

$$c_{eff} = \sqrt{\gamma R_a K} + V_w \cos(\xi - \psi) \tag{5}$$

in which γ is the adiabatic index, R_a is the specific gas constant for air, K is the (local) absolute temperature and V_w is the local horizontal wind speed. The parameters ξ and ψ specify the propagation and wind directions, respectively. In this way, the wind direction relative to the propagation direction is accounted for in the calculation of the sound speed profile, and the azimuthal dependency of the wind field is collapsed into a sound speed profile that only changes with the altitude. This is sometimes referred to as a 2.5-dimensional approximation [36]. In a refractive atmosphere, both the source emission and reception angles change, and more than two points are (obviously) required to define each path. In case of downwind propagation, multiple ground reflected paths may reach the observer in addition to the direct path. In the case of upwind propagation, the shadow zone may prevent the sound from reaching the observer at all (ignoring diffraction). For more details on the auralization of aircraft noise for nonhomogeneous atmospheres, the reader is referred to Arntzen et al. [39].

5.2 Path Traversal

Regardless of whether the auralization follows the time domain or frequency domain approach, a series of propagation effects is applied to the source noise data to produce the noise signatures at the observer. The path traversal operation calculates the propagation effects independently for each path; the effects differ between direct and ground reflected paths, and between straight-line and curved paths. Each effect is time varying for a moving source, and is (re)calculated for each scenario update.

Geometric or spherical spreading accounts for the decrease in noise level associated with propagation from the source to the observer due to the spreading of energy as the sound waves expand into the surrounding air. For a straight-line path, the negative gain (attenuation) is given by reference distance divided by the slant range distance R at the emission time. The reference distance is taken as the radius at which the source noise description is defined. For a curved path, the spreading loss is calculated by the spread of a ray tube bundle from the reference distance to the observer.

The time delay is critical for Doppler simulation and ground plane effects. The manner in which that manifests itself is given in Section 5.3. For a straight-line path, it is simply the speed of sound divided by the slant range distance R at the emission time. For a curved path, the delay is accumulated along each piecewise straight-line propagation segment.

The aircraft sound is additionally attenuated due to absorption by the atmosphere caused by viscous effects and molecular composition. The extent to which the atmosphere absorbs the sound from an aircraft depends on the frequency of the sound as well as the local air temperature and relative humidity. The atmospheric absorption per unit path length (dB/m) is calculated for each straight-line segment at 1/3-octave band center frequencies or pure tone frequencies. The total absorption at each frequency is calculated as the product of the absorption per unit length times the segment length, summed along the entire path. Several standard methods are available for calculating the atmospheric absorption, see refs. [40,41]. In the time domain approach, the resulting absorption spectrum is converted to a finite impulse response (FIR) filter, as described in ref. [3].

Reflections off of a finite impedance boundary, e.g. the ground, change the propagation direction and spectrally attenuate the sound. The reflection is generally considered as specular, so the angle of reflection equals the angle of incidence. In most cases, a plane wave propagation can be assumed, resulting in an attenuation that is a function of frequency and the angle of incidence. For low flying sources, a spherical correction must be applied [42], resulting in an additional dependency on range [43]. The impedance model dictates the frequency dependency of the reflection coefficient, while the wave propagation model (plane or spherical) dictates the angle/range dependency. An often used impedance model by Delany and Bazley [44], uses the effective flow resistance as a single parameter. Other models, notably those by Attenborough [45], offer additional parameters. The resulting attenuation is applied only to the reflected path. In the time domain approach, it is converted to an FIR filter, as described in ref. [43]. A hard surface with infinite impedance will reflect all of the sound that is incident upon it.

Further propagation considerations can also add to the fidelity of the auralized sounds at the observer. The modeling and addition of atmospheric turbulence allows the auralization to more closely resemble measured aircraft sounds [46,47]. Some turbulence modeling approaches have been suggested by Shin et al. [48], Arntzen et al. [7] and Rietdijk et al. [6], for instance.

5.3 Application of Propagation Effects

The above propagation effects can be applied within either a time domain or frequency domain auralization approach; only the manner of implementation differs. Below we focus on the time domain approach and adopt the following shorthand to designate the gain (G), time delay (T), and filter (F). A functional block diagram incorporating all of the above effects, between the synthesized source and the summed output, is shown in Fig. 6. The atmospheric turbulence model indicated follows that described by Rietdijk et al. [6], and includes both a time delay and filter term. The pseudo-recording at the end of the process is a calibrated pressure time history at the designated observer.

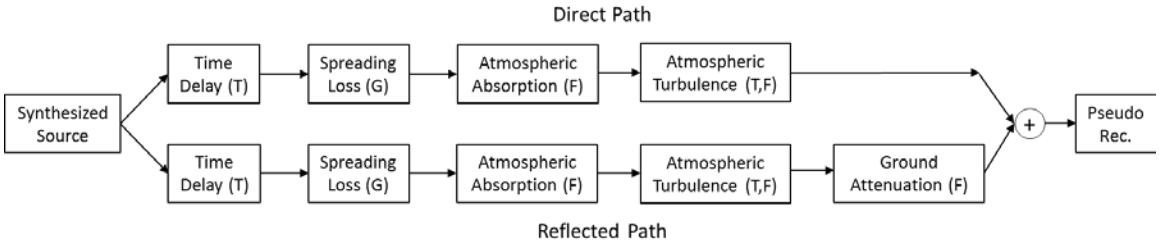

Fig. 6 Functional block diagram depicting application of atmospheric propagation effects for a straight-line propagation path.

The time delay introduces two effects. First, the change of the time delay during the course of the flyover acts to Doppler shift the synthesized source. As the aircraft approaches, T decreases with time. The resulting compression gives rise to a positive pitch shift (Doppler shift factor > 1). As the aircraft retreats, the T increases with time. The resulting stretching gives rise to a negative pitch shift (Doppler shift factor < 1). The second effect is the 'comb-filter' effect, which manifests itself when processed signals associated with the direct and reflected paths are combined. This interference effect is caused by the differing time delays applied to the direct and reflect paths; the time delay of the reflect path being slightly longer than the direct path. The difference in the time delay varies over the course of the flyover and produces the distinctive sound that is also visually apparent in the spectrograms (see the auralization example in Section 7.1).

Fig. 6 gives a representation of how each propagation effect generates its G, T, and F, but does not indicate how these effects are applied in a digital signal processing (DSP) sense. A specific implementation of DSP operations incorporated within the 'Propagate' block of Fig. 3 is shown in Fig. 7. This implementation is embodied in the GTF-processor of the NASA Auralization Framework (NAF) [49]. The inputs to the NAF GTF-processor for each processing time slice are a hop-sized block of synthesized signal and a GTF-series from the path traversal. The GTF-series is the set of linear gains, time delays and filters associated with each path segment. For example, in the case of a straight-line path, there is one GTF specified for the direct path, but a series of two GTFs (source-ground segment and ground-observer segment) for the ground-reflected path. Upon submission, the block of signal is concatenated into a very long delay-line, while the GTF-series is submitted to a FIFO (first-in, first-out) queuing container. When asked to process, the first-out GTF-series in the FIFO queuing container is examined for the amount of signal required to produce a block of output. If enough signal exists in the delay-line, then the GTF-series is processed. A sample interpolator extracts the required samples by the ratio of previous delay to the new delay. Since the time delay is not generally an integer multiple of the audio sampling rate, the fractional delay processing of the sample interpolator must be performed in a manner that avoids audible artifacts, e.g., aliasing of tones. The extracted samples are placed into a work buffer, where they are filtered in-place sequentially by the filter list of the collapsed (linear gains multiplied, time delay summed, and filters enumerated) GTF-series. The samples are scaled by the gain upon copy to an output buffer. The process is repeated until the end of the simulation.

An alternative scheme for GTF processing would be to incorporate the propagation time delay in the synthesized source by specifying a non-uniform source emission time increment such that the arrival of samples at the observer are at equal time increments. Such a strategy is less desirable because it necessitates path traversal ahead of source noise synthesis, whereas those operations may be performed in parallel with the above strategy (see Fig. 3).

Finally, in a frequency domain auralization approach, all of the propagation effects are performed in the frequency domain. Here, the alternative scheme of specifying unequal source emission times, such that the arrival at the observer is in equal time increments, does not suffer the same penalty as the time domain auralization approach, because receiver noise synthesis follows propagation.

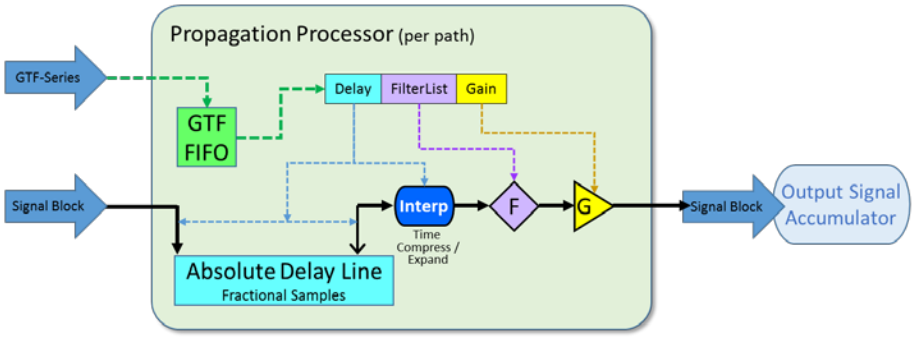

Fig. 7 GTF-processor block diagram used in the NASA Auralization Framework [49].

6 Receiver Considerations

6.1 Listener Simulation

Having generated a calibrated pseudo-recording at the observer, several means are available for presenting the signal to a human subject for evaluation; nonspatialized (monaural) and spatialized (multichannel). The advantage of presenting the sound as spatialized is that it gives the listener additional directional cues aside from those associated with the Doppler shift, changing level, and changing frequency content. These cues allow the sound to be presented in a more natural listening environment, particularly when performed within a real-time interactive environment.

Spatialized sound reproduction may be performed over headphones or over a loudspeaker array. For sound reproduction over headphones, binaural listening is typically simulated by filtering the sound through head related impulse response (HRIR) functions [50]. Here, the HRIRs for the left and right ears are selected based on the receiver angle, as determined from the path calculation, and the listener's instantaneous head orientation, as determined through head tracking. The HRIRs are updated (typically $\geq$ 100 Hz) during the course of the simulated event. The direct and ground reflected paths may be filtered independently (prior to mixing), or may be mixed and presented at only the angle corresponding to the direct path. The latter approach takes advantage of the precedence effect [50], which causes the listener to perceive a single reception angle from the first arriving (direct path) sound when the second (indirect path) sound arrives within a short time interval. Headphone equalization and gain are required to provide a flat response at the calibrated level.

There are several means of reproducing spatialized sound over loudspeaker arrays. These include wave field synthesis, vector base amplitude panning (VBAP), ambisonics, and binaural simulation with cross talk cancellation, see refs. [1,50]. As with headphone reproduction, loudspeaker equalization is required, with additional compensation for gain and time delay for irregular array geometries. Further, many listening venues are limited in their ability to physically locate speakers below the listener, so the precedence effect is often exploited so that sound may be presented along the direct path angle only. An implementation of VBAP is utilized in the NASA Langley Exterior Effects Room (EER) [51], which uses an array of 31 speakers to simulate an outdoor listening environment. Head tracking is not required when the sound is reproduced over loudspeakers because the sound is presented from a fixed position, irrespective of the listener's head orientation.

6.2 Perception-Influenced Design

Noise certifications metrics are used almost exclusively in commercial aircraft design as they present the minimum requirement for noise. These metrics include the maximum A-weighted sound pressure level (SPL), or L_{Amax} for lightweight propeller-driven aircraft, the sound exposure level (SEL) for lightweight helicopters, and the effective perceived noise level (EPNL) for most other aircraft classes [52]. Noise certification regulations utilizing these metrics are based on a balanced approach to manage aircraft noise in the most cost-effective manner. In other words, the regulations do not ensure that the noise exposure is, by any definition, acceptable. Given that aircraft noise design will continue to be based solely on acoustical factors for the foreseeable future and given that current certification requirements are not focused on achieving low annoyance designs, it should be possible to achieve reduced community noise impact by simultaneously meeting noise certification and other design requirements, as well as other acoustic requirements, which directly address human response. This is referred to as perception-influenced design [2].

For vehicle designs or operations that are radically different from the current fleet, auralization plays a crucial role for assessing human response to noise, including annoyance, audibility, sleep or other activity disturbance, etc. In this context, auralized sounds can be used as the stimuli in psychoacoustic tests to determine how well existing metrics

correlate with human response, or to aid in the development of new metrics if existing measures are deficient. These metrics can serve as additional cost functionals in the multidisciplinary analysis and optimization (MDAO) process, as indicated by the feedback loop from the human response and metrics block to the MDAO block in Fig. 8. In the absence of a suitable metric, human response data can also be used directly as a means of assessing the source and its installation, as indicated by the feedback loop to the source noise models and PAA blocks. In short, focusing solely on the certification metrics only ensures that new aircraft will meet noise certification requirements, but that may not lower the community noise impact for residents exposed to their sounds [53].

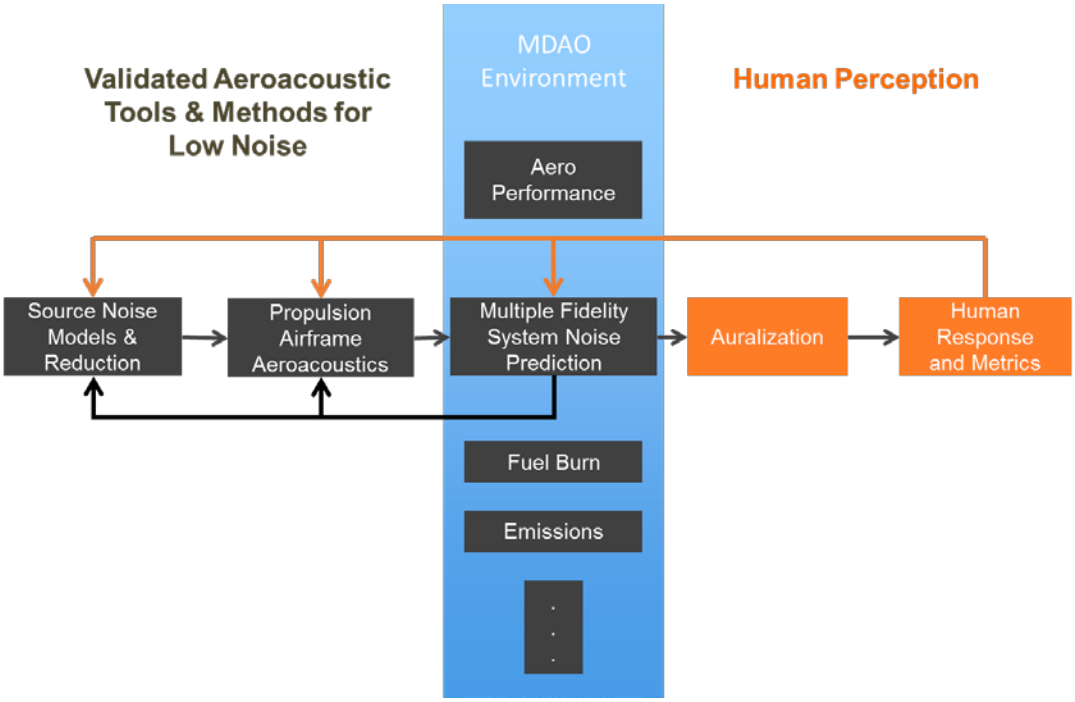

Fig. 8 Components of metrics-driven (black) and perception-influenced (orange) design approaches applied to low-noise aircraft design.

Different models exist for different aspects of human response. Focusing here on annoyance, a well-known model is Zwicker and Fastl's psychoacoustic annoyance model [54], which is based on psychoacoustic tests using narrowband and broadband sounds having different spectral and temporal characteristics. This model has the sound quality metrics of loudness, sharpness, fluctuation strength and roughness as its parameters. More [55] developed a modified psychoacoustic annoyance model using simulated aircraft sounds with controlled sound quality attributes including tonality. He demonstrated that loudness was the dominant model parameter governing annoyance to noise from current fleet transport aircraft, followed by tonality. Further, his model was more highly correlated with annoyance than the applicable EPNL certification metric, which accounts for level and tonal contribution in a different manner. For the radically different distributed electric propulsion (DEP) sounds, a preliminary annoyance model using mean annoyance ratings was developed by Rafaelof [56]. More recently, a model utilizing all subject observations was developed by Rizzi et al. [57] with model parameters consisting of loudness, roughness and tonality.

Perception-influenced design, while made possible by recent advances in auralization, is still in its infancy. Its widespread use is not expected anytime soon. It will take further development of tools and methods, and successful demonstration of the approach on vehicle noise issues that are denying entry into markets, before it is accepted by those directly and indirectly involved in aircraft design.

7 Applications

Recent aircraft noise auralizations across a wide range of vehicle classes are next presented. These were selected to highlight some novel feature associated with each. In the large transport class, the integration with the system noise prediction of turbofan and airframe sources is featured. In the propeller aircraft class, an analytical formulation was used for the isolated source noise predictions, and their superposition is shown to generate unique noise signatures for

DEP configurations. The CROR propulsor example demonstrates the use of wind tunnel test data for the source noise description, while the rotorcraft example demonstrates the use of flight test data and the propagation model effects. Lastly, the small UAS example demonstrates the use of CFD-generated data and the necessity to include flight dynamics modeling for inherently unsteady effects.

7.1 Large transport aircraft

Auralization has been most widely applied to large short-range and long-range civil transport aircraft sounds [10,11,28,32,37,46,47,53,58]. Auralizations of these aircraft sounds, many of which are familiar and which are responsible for the largest portion of community exposure, have been performed for a variety of reasons. These include communicating community noise impact to nonexperts in a more tangible way [37,46], demonstrating the noise benefits of alternate or new engine and airframe technologies [10,11,32], and examining the correlation of annoyance with certification metrics [58]. Transport aircraft noise is comprised of broadband and tonal noise sources, emanating from both the engine and the airframe. This example made use of sound quality metrics to optimize aircraft sounds for potentially lower annoyance and used auralization to present the resulting changes [53]. The study focused on a short-range commercial airliner, similar to an A320-200 aircraft and optimized the aircraft's design for minimal community noise impact in terms of EPNL, loudness and tonality metrics.

The study primarily made use of semi-empirical frequency domain source noise models. The engine sources consisted of broadband jet mixing noise, and broadband fan noise, fan rotor-stator interaction tones, and fan combinations tones. The combination or buzz saw tones do not occur during approach due to low engine thrust setting. Combustor and turbine noise were not included due to their low intensity compared to the fan and jet noise components. Acoustic treatment in the form of inlet and aft acoustic liners was applied to the source noise hemispheres, and the effect of chevron nozzles on jet mixing noise was also modeled. All the major airframe noise sources indicated in Table 5 were modeled. The tonal source noise from the fan was synthesized using the additive synthesis technique discussed in Section 4.2 with random phase for each tone; the broadband noise was synthesized using the subtractive synthesis method discussed in Section 4.1.

The source noise description was determined using semi-empirical source noise models incorporated in the INSTANT module, along departure and approach flight trajectories simulated using the MICADO environment (see Section 3.4). The propagation to the observer was performed using a straight-line propagation approach, following the methodology of Section 5. An observer location directly below the flight path and 25 km before aircraft touchdown at the airport was selected as representative of community noise exposure experienced by residents. The spectrogram for the reference design, expressed by SPL (dB), is shown in Fig. 9 [Audio Sample 1]. The study showed that for the aircraft considered, the design achieved by minimizing the EPNL metric (Fig. 10) was very similar to that achieved by minimizing the loudness (Fig. 11) metric. The design achieved by minimizing the tonality metric (Fig. 12) [Audio Sample 2] reduced the tonal intensity, whilst altering the broadband noise in a way that reduced tonal prominence. This increased tonal masking by low frequency broadband noise components. Each optimized design resulted in a perceptibly different sound at the observer compared to the reference aircraft. Yet to be performed psychoacoustic tests are needed to ascertain if the optimized sounds are indeed perceived as less annoying.

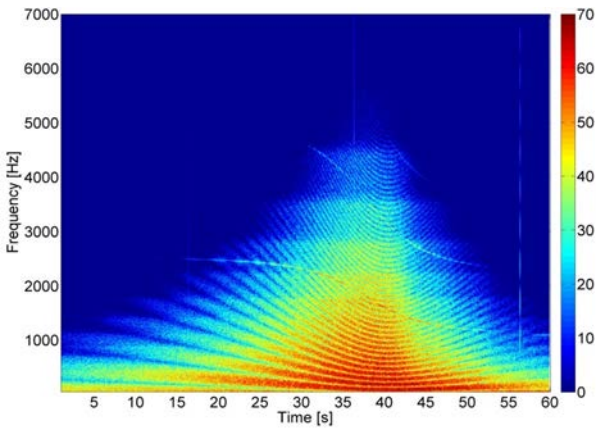

Fig. 9 Short-range transport aircraft spectrogram during approach for the reference design.

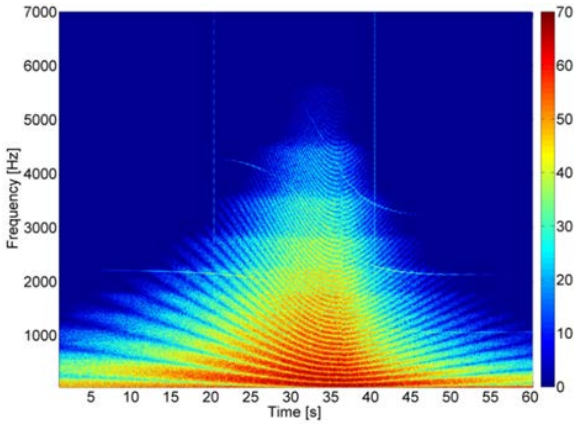

Fig. 10 Short-range transport aircraft spectrogram during approach for the minimum EPNL design.

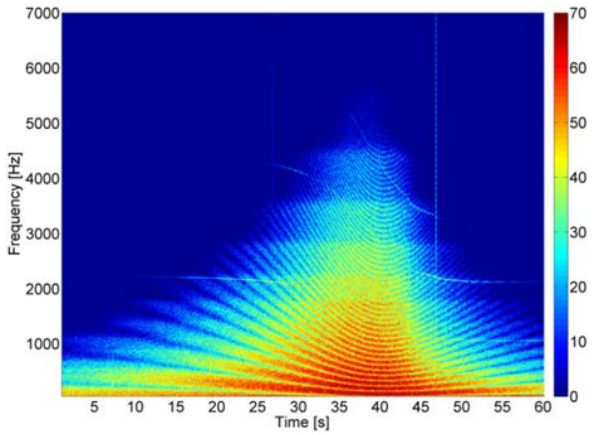

Fig. 11 Short-range transport aircraft spectrogram during approach for minimum loudness design.

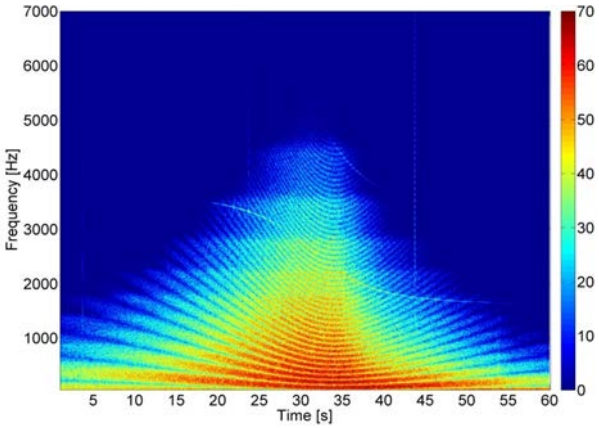

Fig. 12 Short-range transport aircraft spectrogram during approach for the minimum tonality design.

7.2 Distributed electric propulsion aircraft

Design of DEP aircraft configurations for thin haul and small-medium UAS aircraft sectors is on the rise because advances in electric propulsion have opened up new degrees-of-freedom in aerodynamics, vehicle control and acoustics. A DEP concept, called Leading Edge Asynchronous Propellers Technology (LEAPTech), has been a recent research focus at NASA. LEAPTech is a high-lift system that utilizes a large number of low tip speed propellers mounted upstream of the wing leading edge for lift augmentation during low flight speed operations. It is a key technology for the NASA X-57 Maxwell flight demonstrator project [59].

The auralization of noise generated by the high-lift system is not trivial. In addition to both broadband and tonal propeller source noise, there are numerous installation effects including propeller-propeller, propeller-nacelle, and propeller-wing interactions, and other noise sources including electric motor and airframe noise, and wingtip cruise propeller noise. In an exploratory effort, only the tonal components of isolated propeller source noise were included so that early guidance on a spread frequency design strategy might be provided in the absence of a validated annoyance model [57]. The spread frequency strategy is one in which the propellers are operated at somewhat different rotational speeds in order derive some beneficial sound quality. The source noise definition was determined analytically using the Gutin formula [60]. The thickness and loading noise were synthesized with an additive method and propagated to a ground receiver. The superposition of multiple propellers was shown to exhibit unique noise characteristics, both spatially and temporally. When the propellers were synchronized to the same frequency, the spatial distribution on the ground exhibited the highly directive pattern shown in Fig. 13, while the pseudo-recording at a centerline observer was quite regular as shown in Fig. 14 [Audio Sample 3]. When a spread frequency strategy with a 1 Hz change in BPF was employed, it smeared the directivity pattern (see Fig. 15) and highly modulated the pseudo-recording (see Fig. 16) [Audio Sample 4], but the total radiated sound power remained unchanged. The inclusion of electric motor controller error and atmospheric turbulence (not shown) were found to reduce the severity of the modulations.

The auralizations were used as stimuli in a psychoacoustic test to assess and model annoyance [56,57]. It was found that the mean annoyance response varied in a statistically significantly manner with the number of propellers and with the inclusion of time varying effects (motor controller error and atmospheric turbulence), but did not differ significantly with the relative RPM between propellers. An annoyance model was developed using the sound quality metrics of loudness, roughness, and tonality as predictors. With it, new DEP designs may be evaluated to help identify those with low annoyance.

7.3 Contrarotating Open-Rotor Propulsors

The appeal of CROR propulsion systems is their potential for large reductions in fuel burn relative to contemporary turbofan engines. Work in the 1970s and 1980s successfully demonstrated through ground and flight tests that CROR technology could achieve its fuel-burn target with acceptable acoustic performance for the regulations at the time. More recent work, taking advantage of contemporary CFD and computational aeroacoustic tools to optimize blade designs, demonstrated improved aeroperformance and noise reduction through a series of scale model wind-tunnel tests [61]. It was felt that the best way to communicate the remarkable acoustic improvements of the latest generation designs would be through auralization [11].

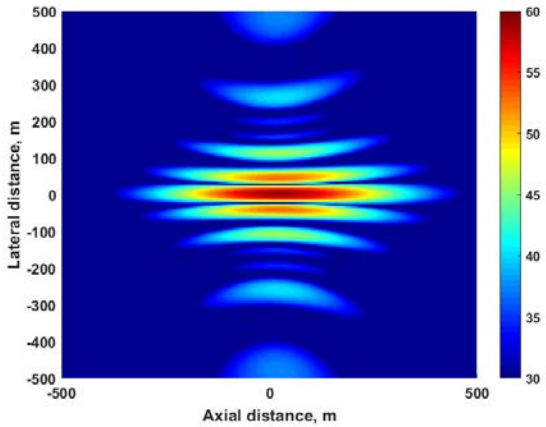

Fig. 13 Sound pressure radiation pattern (dB) for a synchronized 12-propeller configuration.

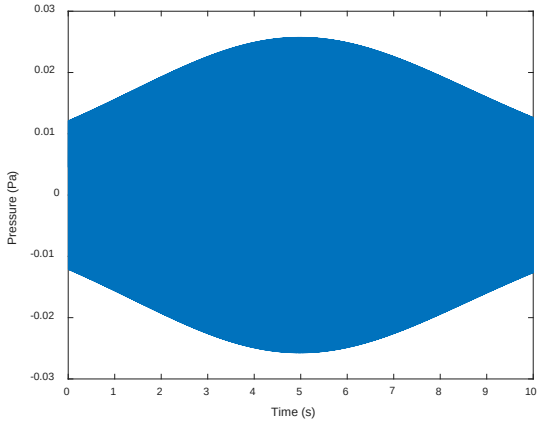

Fig. 14 Pressure time history (Pa) for a flyover of a synchronized 12-propeller aircraft at a centerline observer location.

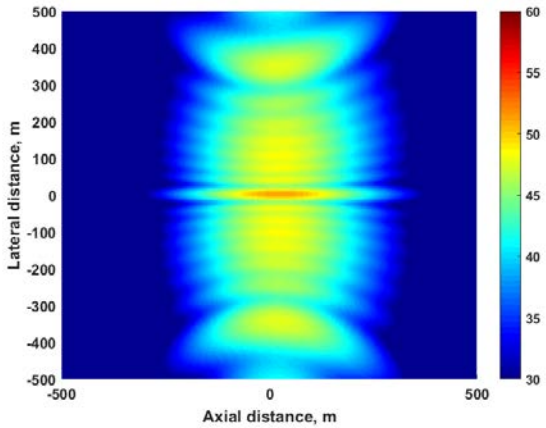

Fig. 15 Sound pressure radiation pattern (dB) for a spread frequency 12-propeller configuration.

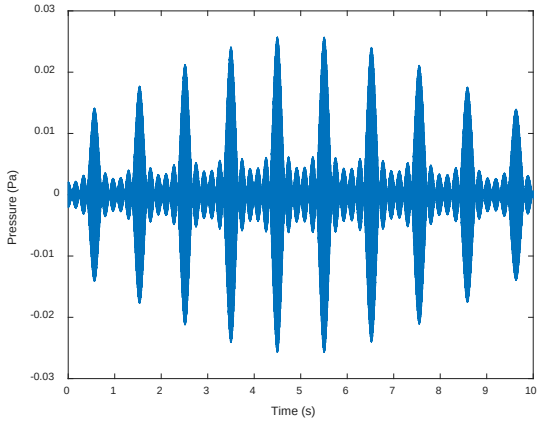

Fig. 16 Pressure time history (Pa) for a flyover of a spread frequency 12-propeller aircraft at a centerline observer location.

Because the source noise prediction models for open-rotor engines are a topic of current research [62], the auralization used the wind-tunnel test data as the basis for the source noise description. This entailed i) converting the scale-model wind-tunnel acoustic data to full scale flight-condition data, using an approach adapted from Guynn et al. [63], and ii) separating coherent tonal noise at the shaft order frequencies from incoherent broadband noise. The resulting tonal source noise definition was synthesized using the additive synthesis method with random phase and the broadband noise was synthesized using the subtractive synthesis method with a narrowband spectrum as its starting point. The two components were summed and propagated to a ground receiver as previously described in a simulated flyover event.

Auralizations were performed to examine the effect of thrust level, propulsor installation (isolated or pylon mounted), rotor-inflow angle, and blade sets. The tone corrected perceived noise level (PNLT) traces for two full-scale thrust settings of the isolated baseline blade set are shown in Fig. 17, along with the emission angle as a function of receiver time. Reading 359 refers to a thrust setting of 13,741 lbf [Audio Sample 5] and reading 361 refers to a thrust setting of 14,650 lbf [Audio Sample 6]. The auralization metrics agree very well with those obtained by propagating the unseparated spectra within ANOPP; EPNL values are within 0.3 dB. To gain some insight into the higher noise levels associated with the higher thrust, it is useful to look at a breakdown of A-weighted SPL and PNLT between tonal and broadband components, as shown in Fig. 18. It is seen that the tonal and broadband contributions are comparable on the approach side, while the retreating side is dominated by the tonal contribution. The source noise separation technique used in this work was subsequently applied to the auralization of geared turbofan engines

[10], for which accurate source noise prediction models also do not yet exist. The reader is directed to the paper on novel engine technologies found in this special issue for the latest source noise prediction methods.

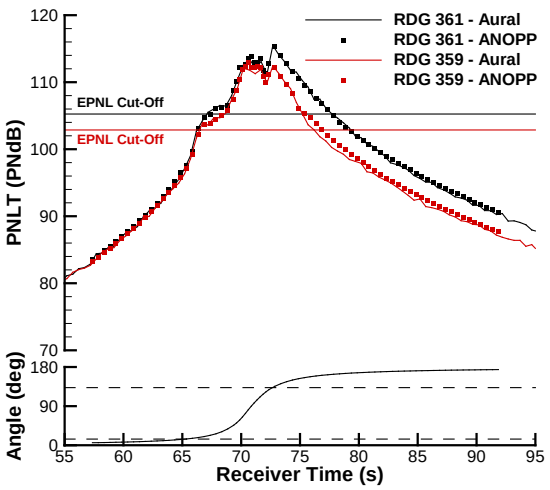

Fig. 17 PNLT for two flyovers with different thrust levels (flush receiver).

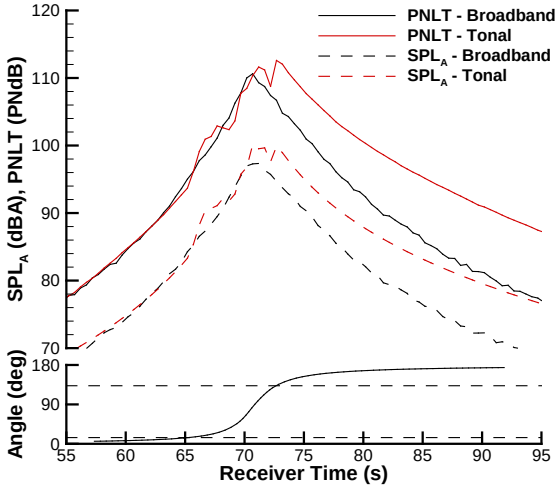

Fig. 18 Breakdown of tonal and broadband metrics from auralization for the higher thrust level.

7.4 Rotorcraft

Noise from low flying rotorcraft is a source of annoyance in both natural and populated areas and is the impetus for recent rules restricting their operations. It has been common practice to acquire ground microphone measurements from rotorcraft flight tests to populate noise hemispheres with 1/3-octave band spectra for noise simulation programs like AAM. More recently, methods have been developed to back propagate [13] and separate the main and tail rotor noise signatures as a function of source emission angle [14]. These noise signatures are in the form of time-averaged pressure time histories for a single blade passage.

A recent auralization of low flying rotorcraft operations [43] was performed using such noise signatures from an Airbus/Eurocopter AS350B “AStar” light utility helicopter. The auralizations served as test stimuli in a psychoacoustic test to assess audibility [64]. Therefore, operations were restricted to those approaching from a great distance and ending well short of overhead angles, that is, a so-called fly-in. For this purpose, it was sufficient to utilize a single source emission angle near the tip path plane, as shown in Fig. 19. The noise signatures of the main and tail rotor were separately analyzed for their magnitude and phase at the BPF harmonics via a DFT, and synthesized using an additive synthesis method. The source noise definition is shown in Fig. 20 for the forward emission angle, and the synthesized pressure time history is shown in Fig. 21 [Audio Sample 7]. Note that because the BPFs of the main and tail rotors are not harmonically related, the synthesized signal does not repeat itself on the interval shown.

The effect of different ground impedances and wave propagation models was also investigated. Three different ground impedances were specified using the Attenborough four-parameter model [45]: packed sandy silt, new asphalt, and grass. Due to the low elevation angle associated with the fly-in, the spherical wave correction was applied to each; the packed sandy silt ground was also modeled using the plane wave assumption. Fig. 22 provides a comparison of overall SPL (OASPL) for each case. The distance is normalized by the mean audibility distance of the packed sandy silt ground with spherical wave propagation (solid black line), as determined through psychoacoustic testing. The differences in OASPL between auralizations decrease with decreasing emission distance. At the farthest range, the difference in OASPL between ground surfaces is as much as 16 dB, between new asphalt and grass. This large effect due to changes in ground impedance illustrates its importance in determining the distance at which audibility will occur, particularly for low frequencies where atmospheric absorption has little effect. The comparison of propagation models indicates that the plane wave model underpredicts the attenuation relative to the spherical wave model at normalized distances greater than 0.4, suggesting that audibility will occur at a substantially greater range and reinforcing the need to select an appropriate propagation model.

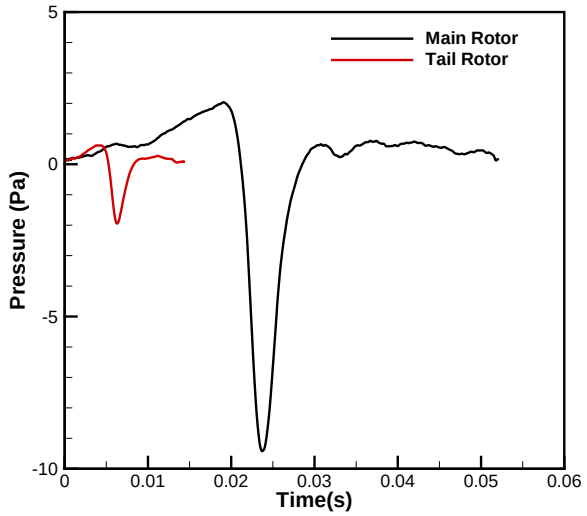

Fig. 19 Time-averaged main & tail rotor signatures.

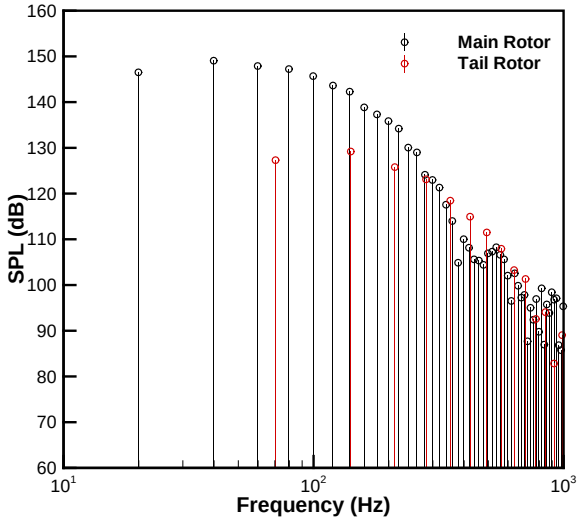

Fig. 20 Harmonics of the main & tail rotor signatures.

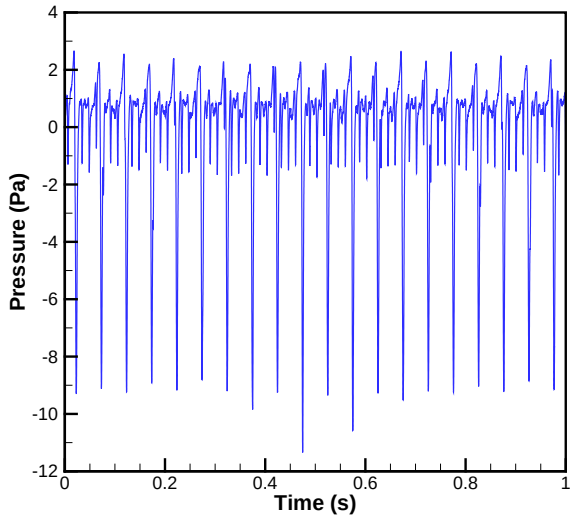

Fig. 21 Snippet of synthesized pressure time history.

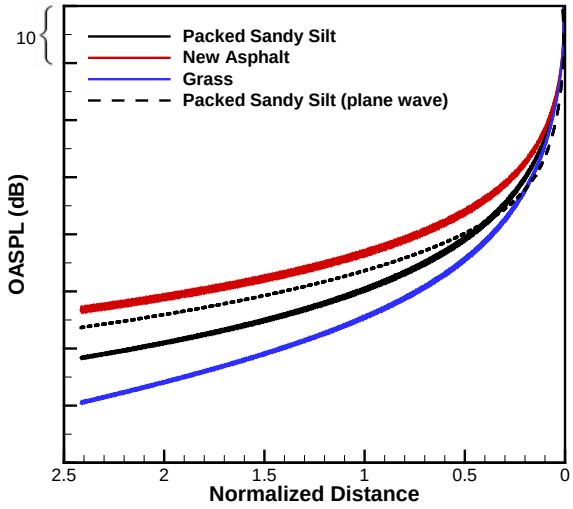

Fig. 22 Comparison of overall SPL for simulated fly-ins with three ground impedances.

7.5 Small UAS

Lastly consider the auralization of a small UAS. Small UAS are being considered for package delivery and are already in use in aerial photography, disaster management, search and rescue, and many other civil applications. Because their numbers are expected to rise dramatically, and because their operations are in close proximity to humans, noise is expecting to become a key issue. Not much work has been done to understand how small UAS vehicle design affects the noise produced or the annoyance to it.

An effort was therefore undertaken to auralize the sound produced by quadcopters [65], so that the distinctive sound they produce could be better understood and appropriate noise mitigation strategies could ultimately be developed. A spectrogram of a recorded flyover from the DJI Phantom 2 quadcopter is shown in Fig. 23 [Audio Sample 8]. (Note that each spectrogram is normalized by its peak, but the dynamic range of both spectrograms in this section is the same.) The BPF and higher harmonics of the front and rear pair of rotors is apparent, as is their variation with time. The auralization utilized a tonal source noise description of a single isolated rotor. The source noise hemisphere of pressure time histories for a single blade passage was obtained from acoustic predictions using CFD-generated blade loadings. Noise from electric motors, broadband noise, and rotor-structure interaction noise were not included in the auralization, see Christian et al. [66] for additional details on the source noise description. Each

pressure time history on the hemisphere was analyzed using a DFT to obtain the associated magnitude and phase. These were spatially interpolated and used to synthesis the source noise using an additive synthesis approach and propagated to a ground receiver a short distance away.

A quadcopter flight dynamics model was used to obtain the individual rotor speeds used to set their BPFs. Most such models include only basic flight dynamics. The model used did not include drag or turbulence. Consequently, once the quadcopter obtained the desired speed, the vehicle followed a straight and level trajectory with all rotors operating at the same speed. The unrealistic flight condition resulted in an unrealistic auralization, [Audio Sample 9]. The baseline model was extended to include body and rotor drag, turbulence, and manufacturing error [65]. The addition of body and rotor drag had the effect of separating the front and rear rotor BPFs, [Audio Sample 10]. The resulting pitched attitude of the vehicle also changed the emission angle (and to a small extent, the slant range). The addition of turbulence to the drag introduced unsteadiness [Audio Sample 11]. Finally, the addition of manufacturing error, introduced using a normally distributed error of 10% in the thrust coefficient of the four rotors, produced the spectrogram shown in Fig. 24 [Audio Sample 12]. Here it is seen that, like the recording, the two rear motors are split in frequency by a smaller amount than the two front rotors. This comes about because the more rapidly spinning rear rotors require less of a change in speed to overcome the same magnitude change in thrust coefficient than the slower spinning front rotors.

This example demonstrates the need to incorporate the appropriate unsteady flight dynamics effects for small vehicles that do not fly in a trimmed condition. Some of these auralizations were subsequently used as test stimuli in a psychoacoustic test to investigate annoyance from small UAS noise [67].

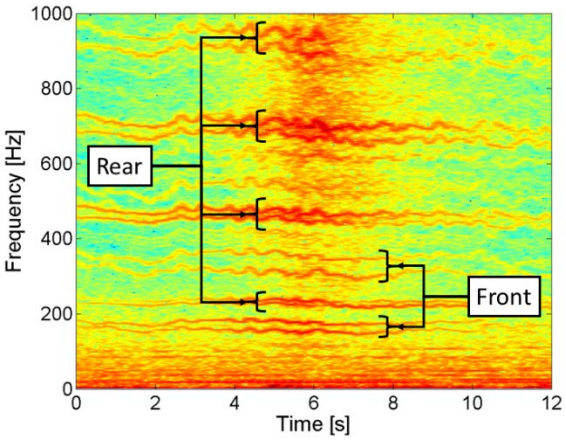

Fig. 23 Spectrogram of recorded quadcopter flyover.

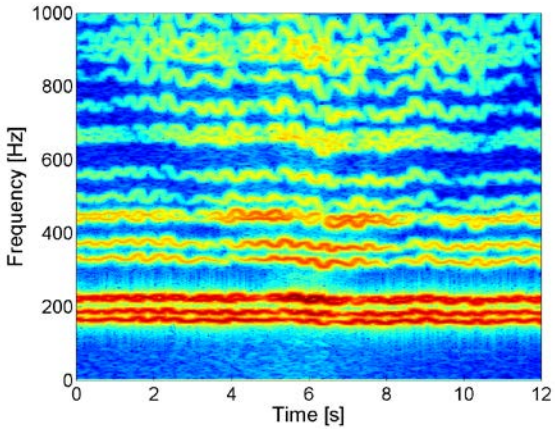

Fig. 24 Spectrogram of auralization including the effects of drag, turbulence and manufacturing error.

8 Concluding Remarks

Work over the last decade plus has advanced the maturity of auralization of air vehicle noise. Many of the constituent methods for simulating the source, path, and receiver have been developed and applied to a wide range of conventional and unconventional configurations, spanning small UAS to large commercial transports.

As pointed out, there are additional developments to undertake. In the area of source noise synthesis, the handling of aperiodic source noise definitions remains largely unaddressed. In order to make auralization more accessible, better tool integration is needed, particular between the source noise definition and the synthesis. Some advancements have been made in this area, e.g., the ANOPP2-NAF interface [68], but much more work remains. Doing so will allow better leveraging of constituent capabilities, e.g., utilization of advanced propagation models in AAM for the path calculation and path traversal. The capabilities of such programs to generate predictions at the observer also serve as incentives to further develop the less commonly used frequency domain approach.

Lastly, auralization technology has advanced to the degree that it has because new applications have driven its development. The existing issues with annoyance to rotorcraft noise and the emerging issues with respect to small UAS and UAM vehicles will necessitate higher fidelity simulations to support development of annoyance models for perception-influenced design. Efforts directed at the vehicle operations away from airports, e.g., urban canyons, will further stimulate advancements in sound propagation needed for auralization in these environments.

References

1. Vorländer, M.: Auralization - Fundamentals of acoustics, modelling, simulation, algorithms and acoustic virtual reality. Springer-Verlag, Berlin (2008)
2. Rizzi, S.A.: Toward reduced aircraft community noise impact via a perception-influenced design approach. In: InterNoise 2016, Hamburg, Germany, pp. 2-26 (2016)
3. Rizzi, S.A., Sullivan, B.M.: Synthesis of virtual environments for aircraft community noise impact studies, AIAA-2005-2983. In: 11th AIAA/CEAS Aeroacoustics Conference, Monterey, CA (2005)
4. Allen, M.P., Rizzi, S.A., Burdisso, R., Okcu, S.: Analysis and synthesis of tonal aircraft noise sources, AIAA-2012-2078. In: 18th AIAA/CEAS Aeroacoustics Conference, Colorado Springs, CO (2012)
5. Pera, N.M., Rizzi, S.A., Krishnamurthy, S., Fuller, C.R., Christian, A.W.: Development of a method for analysis and incorporation of rotorcraft fluctuation in synthesized flyover noise. In: AIAA SciTech Forum, Kissimmee, FL (2018)
6. Rietdijk, F., Forssén, J., Heutschi, K.: Generating sequences of acoustic scintillations. Acta Acustica United with Acustica **103**(2), 331-338 (2017). doi:10.3813/AAA.919061
7. Arntzen, M., Simons, D.G.: Ground reflection with turbulence induced coherence loss in flyover auralization. International Journal of Aeroacoustics **13**(5-6), 449-462 (2014). doi:10.1260/1475-472X.13.5-6.449
8. Aumann, A.R., Rizzi, S.A.: An atmospheric turbulence model plugin for the NASA auralization framework. In: 173rd Meeting of the Acoustical Society of America and the 8th Forum Acusticum, Boston, MA (2017)
9. Dahl, M.D. (ed.) Assessment of NASA's aircraft noise prediction capability. NASA TP-2012-215653, (2012)
10. Rizzi, S.A., Burley, C.L., Thomas, R.H.: Auralization of NASA N+2 aircraft concepts from system noise predictions, AIAA 2016-2906. In: 22nd AIAA/CEAS Aeroacoustics Conference, Lyon, France (2016)
11. Rizzi, S.A., Stephens, D.B., Berton, J.J., Van Zante, D.E., Wojno, J.P., Goerig, T.W.: Auralization of flyover noise from open rotor engines using model scale test data. AIAA Journal of Aircraft **53**(1), 117-128 (2016). doi:DOI: 10.2514/1.C033223
12. Brentner, K.S., Farassat, F.: Modeling aerodynamically generated sound of helicopter rotors. Progress in Aerospace Sciences **39**(2), 83-120 (2003). doi:http://dx.doi.org/10.1016/S0376-0421(02)00068-4
13. Hobbs, C., Page, J.: Acoustic repropagation technique and practical source characterization for simulation noise model databases. Journal of the Acoustical Society of America **127**(3), 1834 (2010). doi:10.1121/1.3384278
14. Greenwood, E., Schmitz, F.H.: Separation of main and tail rotor noise from ground-based acoustic measurements. AIAA Journal of Aircraft **51**(2), 464-472 (2014). doi:10.2514/1.C032046
15. Thomas, R.H., Burley, C.L., Nickol, C.L.: Assessment of the noise reduction potential of advanced subsonic transport concepts for NASA's Environmentally Responsible Aviation Project, AIAA-2016-0863. In: 54th AIAA Aerospace Sciences Meeting, San Diego, CA (2016)
16. Zawodny, N.S., Boyd Jr., D.D.: Investigation of rotor-airframe onteraction noise associated with small-scale rotary-wing unmanned aircraft systems. In: 73rd Annual AHS Forum, Ft. Worth, TX (2017)
17. Zorumski, W.E.: Aircraft noise prediction program theoretical manual. NASA TM-83199 (1982)
18. Lopes, L.V., Burley, C.L.: ANOPP2 User's Manual: Version 1.2. NASA TM-2016-219342 (2016)
19. Bertsch, L., Isermann, U.: Noise prediction toolbox used by the DLR aircraft noise working group. In: InterNoise 2013, Innsbruck, Austria, (2013)
20. LeGriffon, I.: Aircraft noise modelling and assessment in the IESTA program with focus on engine noise. In: 22nd International Congress on Sound and Vibration (ICSV22), Florence, Italy, (2015)
21. Risse, K., Schäfer, K., Schültke, F., Stumpf, E.: Central Reference Aircraft data System (CeRAS) for research community. CEAS Aeronautical Journal **7**(1), 121-133 (2016). doi:10.1007/s13272-015-0177-9
22. McCullers, L.A.: Aircraft configuration optimization including optimized flight profiles. In: Recent experiences in multidisciplinary analysis and optimization, Part 1, Hampton, VA, pp. 395-412. NASA CP-2327 (1984)
23. Werner-Westphal, C., Heinze, W., Horst, P.: Multidisciplinary integrated preliminary design applied to future green aircraft configurations, AIAA-2007-655. In: 45th AIAA Aerospace Sciences Meeting and Exhibit. AIAA (2007)
24. Johnson, W.: Technology drivers in the development of CAMRAD II. In: AHS Aeromechanics Specialists Conference, San Francisco, CA (1994)
25. Lytle, J.K.: The numerical propulsion system simulation: an overview. NASA TM-2000-209915 (2000)
26. Visser, W., Broomhead, M.: GSP - A generic object oriented gas turbine simulation environment. National Aerospace Laboratory (NLR), The Netherlands (2000)
27. Kurzke, J.: GasTurb 11 Users Manual - A program to calculate design and off-design performance of gas turbines. GasTurb GmbH, Institute of Jet Propulsion and Turbomachinery of RWTH Aachen University (2007)
28. Sahai, A.K., Stumpf, E.: Incorporating and minimizing aircraft noise annoyance during conceptual aircraft design, AIAA-2016-2906. In: 20th AIAA/CEAS Aeroacoustics Conference, Atlanta, GA. AIAA AVIATION Forum (2014)
29. Heath, C., Gray, J.: OpenMDAO: Framework for flexible multidisciplinary design, analysis and optimization methods, AIAA-2012-1673. In: 53rd AIAA/ASME/ASCE/AHS/ASC Structures, Structural Dynamics and Materials Conference. AIAA (2012)
30. Johnson, W.: NDARC, NASA design and analysis of rotorcraft. NASA TP-2015-218751 (2015)
31. Page, J.A., Wilmer, C., Schultz, T., Plotkin, K.J., Czech, J.: Advanced acoustic model technical reference and user manual, SERDP Project WP-1304. Wyle Laboratories, Inc. (2009)

32. Rizzi, S.A., Aumann, A.R., Lopes, L.V., Burley, C.L.: Auralization of hybrid wing-body aircraft flyover noise from system noise predictions. AIAA Journal of Aircraft **51**(6), 1914-1926 (2014). doi:10.2514/1.C032572
33. Rietdijk, F., Heutschi, K.: Auralization of aircraft noise in an urban environment. In: InterNoise 2016, Hamburg, Germany, pp. 2877-2881 (2016)
34. Farassat, F.: Derivation of formulations 1 and 1A of Farassat. NASA TM-2007-214853 (2007)
35. Farassat, F.: Theory of noise generation from moving bodies with an application to helicopter rotors. NASA TR R 451 (1975)
36. Arntzen, M.: Aircraft noise calculation and synthesis in a non-standard atmosphere, Ph.D. Thesis, Faculty of Aerospace Engineering. TU Delft, Delft, The Netherlands (2014)
37. Sahai, A., Anton, E., Stumpf, E., Wefers, F., Vorlaender, M.: Interdisciplinary auralization of take-off and landing procedures for subjective assessment in virtual reality environments, AIAA-2012-2077. In: 18th AIAA/CEAS Aeroacoustics Conference, Colorado Springs, CO (2012)
38. Sahai, A., Wefers, F., Pick, S., Stumpf, E., Vorländer, M., Kuhlen, T.: Interactive simulation of aircraft noise in aural and visual virtual environments. Applied Acoustics **101**, 24-38 (2016). doi:10.1016/j.apacoust.2015.08.002
39. Arntzen, M., Rizzi, S.A., Visser, H.G., Simons, D.G.: A framework for simulation of aircraft flyover noise through a non-standard atmosphere. AIAA Journal of Aircraft **51**(3), 956-966 (2014). doi:10.2514/1.C032049
40. Acoustics - Attenuation of sound during propagation outdoors - Part 1: Calculation of absorption of sound by the atmosphere, ISO-9613-1:1993(E). International Organization for Standardization (ISO) (1993)
41. American National Standard Method for the calculation of the absorption of sound by the atmosphere. ANSI S1.26-1995 (1995)
42. Piercy, J.E., Embleton, T.F.W., Sutherland, L.C.: Review of noise propagation in the atmosphere. Journal of the Acoustical Society of America **61**(6), 1403-1418 (1977). doi:10.1121/1.381455
43. Rizzi, S.A., Christian, A.: A method for simulation of rotorcraft fly-in noise for human response studies. In: InterNoise 2015, San Francisco, CA (2015)
44. Delany, M.E., Bazley, E.N.: Acoustical properties of fibrous absorbent materials. Applied Acoustics **3**(2), 105-116 (1970). doi:10.1016/0003-682X(70)90031-9
45. Attenborough, K.: Acoustic impedance models for outdoor ground surfaces. Journal of Sound and Vibration **99**(4), 521-544 (1985).
46. Arntzen, M., Simons, D.G.: Modeling and synthesis of aircraft flyover noise. Applied Acoustics **84**, 99-106 (2014). doi:10.1016/j.apacoust.2013.09.002
47. Sahai, A.K., Simons, D.G.: Quantifying the audible differences in measured and auralized aircraft sounds, AIAA 2016-2906. In: 22nd AIAA/CEAS Aeroacoustics Conference, Lyon, France (2016)
48. Shin, H.-C., Hall, C., Crichton, D.: Auralisation of turbofan engine noise components, AIAA-2006-2620. In: 12th AIAA/CEAS Aeroacoustics Conference, Cambridge, MA (2006)
49. Aumann, A.R., Tuttle, B.C., Chapin, W.L., Rizzi, S.A.: The NASA Auralization Framework and Plugin Architecture. In: InterNoise 2015, San Francisco, CA (2015)
50. Begault, D.R.: 3-D sound for virtual reality and multimedia. Academic Press, Inc., Chestnut Hill, MA (1994)
51. Faller II, K.J., Rizzi, S.A., Aumann, A.R.: Acoustic performance of a real-time three-dimensional sound-reproduction system. NASA TM-2013-218004 (2013)
52. Annex 16 to the Convention on International Civil Aviation, Environmental Protection, Volume I, Aircraft Noise (7th Edition). In., p. 236. International Civil Aviation Organization, Montreal, Canada, (2014)
53. Sahai, A.K., Snellen, M., Simons, D.G., Stumpf, E.: Aircraft design optimization for lowering community noise exposure based on annoyance metrics. Journal of Aircraft, 1-13 (2017). doi:10.2514/1.C034009
54. Zwicker, E., Fastl, H.: Psychoacoustics, Facts and Models, Second ed. Springer series in Information Sciences. Springer-Verlag, Berlin (1999)
55. More, S.R.: Aircraft noise characteristics and metrics. Ph.D. dissertation, Purdue University (2010)
56. Rafaelof, M.: A model to gauge the annoyance due to arbitrary time-varying sound, Paper 68. In: NOISE-CON 2016, Providence, RI (2016)
57. Rizzi, S.A., Palumbo, D.L., Rathsam, J., Christian, A.W., Rafaelof, M.: Annoyance to noise produced by a distributed electric propulsion high-lift system, AIAA-2017-4050. In: 23rd AIAA/CEAS Aeroacoustics Conference, Denver, CO (2017)
58. Rizzi, S.A., Christian, A.: A psychoacoustic evaluation of noise signatures from advanced civil transport aircraft. In: 22nd AIAA/CEAS Aeroacoustics Conference, Lyon, France (2016)
59. Patterson, M.D., Derlaga, J.M., Borer, N.K.: High-lift propeller system conguration selection for NASA's SCEPTOR distributed electric propulsion flight demonstrator. In: 16th AIAA Aviation Technology, Integration, and Operations Conference, Washington, DC (2016)
60. Gutin, L.: On the sound of a rotating propeller. NACA TM-1195 (1948)
61. Van Zante, D.E., Collier, F., Orton, A., Khalid, S.A., Wojno, J.P., Wood, T.H.: Progress in open rotor propulsors: The FAA/GE/NASA open rotor test campaign. The Aeronautical Journal **118**(1208), 1181-1213 (2014).
62. Envia, E.: Open rotor aeroacoustic modelling. In: Conference on Modelling Fluid Flow (CMFF'12), The 15th International Conference on Fluid Flow Technologies, Budapest, Hungary (2012)
63. Guynn, M.D., Berton, J.J., Haller, W.J., Hendricks, E.S., Tong, M.T.: Performance and environmental assessment of an advanced aircraft with open rotor propulsion. NASA TM-2012-217772 (2012)
64. Rizzi, S.A., Christian, A.W., Rafaelof, M.: A laboratory method for assessing audibility of rotorcraft fly-in noise. In: 73rd AHS Forum, Fort Worth, TX (2017)

65. Christian, A.W., Lawrence, J.: Initial development of a quadcopter simulation environment for auralization. In: 72nd AHS Forum, West Palm Beach, FL (2016)
66. Christian, A., Boyd Jr., D.D., Zawodny, N.S., Rizzi, S.A.: Auralization of tonal rotor noise components of a quadcopter flyover. In: InterNoise 2015, San Francisco, CA (2015)
67. Christian, A.W., Cabell, R.: Initial investigation into the psychoacoustic properties of small unmanned aerial system noise, AIAA-2017-4051. In: 23rd AIAA/CEAS Aeroacoustics Conference, Denver, CO (2017)
68. Tuttle, B.C., Aumann, A.R., Rizzi, S.A., Jones, J., Lopes Jr, L.V.: Flyover noise simulation using NASA's coupled aircraft system noise prediction and auralization frameworks. In: Noise-Con 2017, Grand Rapids (2017)

List of Audio Samples

Audio Sample 1 Auralization of short-range commercial transport reference design on approach.

Audio Sample 2 Auralization of short-range commercial transport minimum tonality design on approach.

Audio Sample 3 Auralization of a flyover of a synchronized 12-propeller aircraft.

Audio Sample 4 Auralization of a flyover of a spread frequency 12-propeller aircraft.

Audio Sample 5 Auralization of a flyover of a contrarotating open-rotor propulsor at a thrust setting of 13,741 lbf.

Audio Sample 6 Auralization of a flyover of a contrarotating open-rotor propulsor at a thrust setting of 14,650 lbf.

Audio Sample 7 Synthesized helicopter source noise at a shallow emission angle.

Audio Sample 8 Recorded flyover of a DJI Phantom 2 quadcopter.

Audio Sample 9 Auralization of a quadcopter using baseline flight dynamics model.

Audio Sample 10 Auralization of a quadcopter using modified flight dynamics model with body and rotor drag.

Audio Sample 11 Auralization of a quadcopter using modified flight dynamics model with drag and turbulence.

Audio Sample 12 Auralization of a quadcopter using modified flight dynamics model with drag, turbulence, and manufacturing error.